Brain Struct Funct (2012) 217:37–48
DOI 10.1007/s00429-011-0331-z

ORIGINAL ARTICLE

Glutamatergic input from specific sources influences the nucleus accumbens-ventral pallidum information flow

Edit Papp · Zsolt Borhegyi · Ryohei Tomioka · Kathleen S. Rockland · István Mody · Tamás F. Freund

Received: 8 February 2011 / Accepted: 16 May 2011 / Published online: 5 June 2011

Abstract The nucleus accumbens (NAc) is positioned to integrate signals originating from limbic and cortical areas and to modulate reward-related motor output of various goal-directed behaviours. The major target of the NAc GABAergic output neurons is the ventral pallidum (VP). VP is part of the reward circuit and controls the ascending mesolimbic dopamine system, as well as the motor output structures and the brainstem. The excitatory inputs governing this system converge in the NAc from the prefrontal cortex (PFC), ventral hippocampus (vHC), midline and intralaminar thalamus (TH) and basolateral nucleus of the amygdala (BLA). It is unclear which if any of these afferents innervate the medium spiny neurons of the NAc, that project to the VP. To identify the source of glutamatergic afferents that innervate neurons projecting to the VP, a dual-labelling method was used: *Phaseolus vulgaris leucoagglutinin* for anterograde and EGFP-encoded adenovirus for retrograde tract-tracing. Within the NAc, anterogradely labelled BLA terminals formed asymmetric synapses on dendritic spines that belonged to medium spiny neurons retrogradely labelled from the VP. TH terminals also formed synapses on dendritic spines of NAc neurons projecting to the VP. However, dendrites and dendritic spines retrogradely labelled from VP received no direct synaptic contacts from afferents originating from mPFC and vHC in the present material, despite the large number of fibres labelled by the anterograde tracer injections. These findings represent the first experimental evidence for a selective glutamatergic innervation of NAc neurons projecting to the VP. The glutamatergic inputs of different origin (i.e. mPFC, vHC, BLA, TH) to the NAc might thus convey different types of reward-related information during goal-directed behaviour, and thereby contribute to the complex regulation of nucleus accumbens functions.

Keywords Glutamate · Prefrontal cortex · Hippocampus · Nucleus accumbens · Basolateral amygdala · Midline and intralaminar thalamus

E. Papp (✉) · Z. Borhegyi · T. F. Freund
Laboratory of Cerebral Cortex Research, Institute of Experimental Medicine, Hungarian Academy of Sciences, H-1450 Budapest, P.O. Box 67, Budapest, Hungary
e-mail: papp.edit@koki.hu

Z. Borhegyi · R. Tomioka
Center for Brain Research, Medical University of Vienna, Vienna, Austria

K. S. Rockland
Picower Inst. Learning and Memory, RIKEN-MIT Center for Neural Circuit Genetics, MIT, Cambridge, MA 02139, USA

I. Mody
Department of Neurology and Physiology, The David Geffen School of Medicine, University of California, Los Angeles, CA 90095, USA

Abbreviations

NAc	Nucleus accumbens
mPFC	Medial prefrontal cortex
vHC	Ventral hippocampus
BLA	Basolateral amygdala
PVT	Paraventricular thalamic nucleus
VP	Ventral pallidum
VTA	Ventral tegmental area
PB	Phosphate buffer
TBS	Tris-buffered saline
PHAL	Phaseolus vulgaris leucoagglutinin
EGFP	Enhanced green fluorescent protein AdSynEGFP adenovirus vector using a neuron-specific synapsin I Promoter and enhanced green fluorescent protein reporter (EGFP)

vGluT2 Vesicular glutamate transporter 2 (also known DNPI, Slc17a6)
TH Midline and intralaminar thalamus

Introduction

The nucleus accumbens (NAc), also known as the ventral striatum, participates in higher order brain functions, including reward-related behaviours, motivation, learning and memory and has been considered as an interface between the limbic and motor systems (Mogenson et al. 1980). Dysfunctions of this region may be involved in conditions such as schizophrenia, drug addiction and other neuropsychiatric disorders (Koob and Bloom 1988; O'Donnell and Grace 1998).

The NAc has two major subregions—the shell and the core—defined by histochemical, electrophysiological, connectivity and cellular criteria (O'Donnell and Grace 1993; Jongen-Relo et al. 1994). This structure receives glutamatergic projections from the ventral hippocampus (vHC) (DeFrance et al. 1985), which is involved in generating context, task attention and emotion (Fanselow and Dong 2010); the basolateral nucleus of the amygdala (BLA) (Groenewegen et al. 1980; McDonald 1991), which mediates emotional behaviour; and the prefrontal cortex (Fuller et al. 1987), which modulates activity throughout the limbic system to enable behavioural flexibility. The paraventricular nucleus of the thalamus (PVT) a part of midline and intralaminar thalamus, which is implicated in behavioural responses to psychostimulant drugs (Deutch et al. 1998; Young and Deutch 1998) and the regulation of autonomic and visceral functions (Bhatnagar and Dallman 1999), particularly in response to stress (Bhatnagar et al. 2000), also projects to the shell region of the NAc.

The NAc is the target of a dense dopaminergic innervation arising from the ventral tegmental area (VTA), which is involved in incentive motivation. Dopamine is critical in the NAc in modulating goal-directed behaviour (Kelley and Berridge 2002). The NAc has a major projection to the ventral pallidum (VP) (Heimer et al. 1987; Usuda et al. 1998) that in turn sends its GABAergic projection to the VTA. Mogenson et al. proposed that NAc projections to the VP translated limbic motivation signals into motor output (Mogenson et al. 1980). However, transferring input from NAc to brainstem motor-related targets is only one feature of VP connectivity. The VP is also a central point of convergence for inputs from the orbitofrontal cortex, prefrontal and infralimbic cortex, the amygdala and other structures related to reward. Conversely, the VP projects back to nearly all of its input sources including the NAc for reciprocal information exchange (Haber et al. 1985; Groenewegen et al. 1993). The VP also sends its efferents to the mediodorsal thalamic nucleus (MD). The MD then projects to the mPFC which in turn projects onto the NAc, thereby closing the reward circuit. This circuit plays a role in several aspects of motivational and cognitive behaviour.

Our aim was to study which, if any, of the different excitatory inputs (mPFC, vHC, TH, BLA) terminating on medium spiny neurons of NAc innervate those neurons that project to the VP. To identify the source of glutamatergic afferents that innervate neurons projecting to the VP, a double-labelling method was used: *Phaseolus vulgaris leucoagglutinin* (*PHAL*) for anterograde and EGFP-encoded adenovirus (AdSynEGFP) for retrograde tract-tracing. VGluT2 (vesicular glutamate transporter 2) was used as a global marker for thalamic terminations.

Materials and methods

Animal housing and surgery

25 male *Wistar rats* (Charles-River, Hungary; 200–300 g) were used for *PHAL*-AdSynEGFP tracing experiments (10 for mPFC, 10 for vHC, 5 for BLA tracing) and seven for the AdSynEGFP tracing-vGluT2 labelling in this study. Experiments were carried out according to the guidelines of the Institutional ethical code and the Hungarian Act of Animal Care and Experimentation (1998. XXVIII. Section 243/1998.), in accordance with the National Institutes of Health Guide for Care and Use of Laboratory Animals.

To visualize both the glutamatergic inputs to the nucleus accumbens as well as neurons in the nucleus accumbens projecting to the ventral pallidum, a double-labelling protocol was used. The anterograde tracer Phaseolus vulgaris leucoagglutinin [*PHAL*;Vector Labs, Burlingame, CA, USA; 2.5% in 0.1 M phosphate buffer (PB), 5 μA, 7 s on/off for 20 min)] (Gerfen and Sawchenko 1984) was injected iontophoretically into three targets: the prefrontal cortex, the ventral hippocampus, or the basolateral amygdala to label the afferents. The neurons in the NAc projecting to the ventral pallidum were retrogradely labelled by an adenovirus vector using a neuron-specific promoter synapsin I and enhanced green fluorescent protein (EGFP) reporter (AdSynEGFP) (Tomioka and Rockland 2006). For AdSynEGFP, 1.0 μl was pressure injected through a 10 μl Hamilton syringe, at 1.0 × 1,012 pfu/ml, at BSL2 level (Ichinohe et al. 2008).

Several injections were delivered into the mPFC or vHC or BLA and the ventral pallidum to give produce a strong labelling that was as completely extensive as possible. Stereotaxic coordinates for the injections were determined

using the atlas of Paxinos and Watson (Paxinos 1998) as a reference: for injections of mPFC: anterior-posterior (AP): 3.24, lateral (L): 0.6, dorso-ventral (DV): 1.5–3.3; vHC: (AP): −5.0 (L): 5.2, (DV): 5.6–7.1; BLA: (AP): −2.3, (L): 5, (DV): 6.8–7.2; VP: (AP): −0.7, (L): 3.2, (DV): 7.2–7.9. For surgery, rats were deeply anaesthetized with an intraperitoneal injection of an anaesthetic mixture Equitesin (containing 2.5% ketamine, 0.5% xylazine-hydrochloride, 0.25% promethazinium-chloride, 0.0025% benzetonium-chloride, and 0.002% hydrochinon) used at 0.2 ml/100 g body weight.

Perfusion and preparation of tissue sections

After 2 weeks' survival time the animals were deeply anaesthetized using Equitesin and perfused through the heart first with saline (2–3 min) followed by a fixative containing 2% paraformaldehyde (Sigma) and 0.5% glutaraldehyde (TAAB) in 0.1 M sodium acetate buffer (pH: 6.5) for 2 min, followed by 2% paraformaldehyde/0.5% glutaraldehyde in 0.1 M sodium borate buffer (pH: 8.5) for 1 h (Sloviter et al. 2001). Brains were removed from the skull. Blocks of the NAc and also the injection sites were sectioned on a Vibratome at 60 μm, washed several times in 0.1 M PB, cryoprotected in 30% sucrose in 0.1 M PB overnight and freeze-thawed in an aluminum foil boat over liquid nitrogen four times to enhance the penetration of the antisera.

Immunocytochemistry

The sections were processed for immunoperoxidase, modified immunoperoxidase (Dobo et al. 2011), or preembedding immunogold staining. Subsequently, all washing steps and dilutions of the antibodies were done in 0.05 M TBS, pH 7.4. After extensive washing in TBS, the sections were blocked in 3% bovine serum albumin for 45 min and then incubated in goat anti-*PHAL* (Vector, 1:10,000) antibody for a minimum of 48 h at 4°C. Following the primary antiserum, the sections were treated with biotinylated anti-goat IgG (1:300) for 2 h and then with avidin biotinylated–horseradish peroxidase complex (1:500; Elite ABC; Vector Laboratories) for 1.5 h. The immunoperoxidase reaction was developed using 3, 3′-diaminobenzidine with ammonium nickel sulphate (DAB-Ni) as the chromogen, and then post-intensified with silver-gold (Dobo et al. 2011). After the first immunostaining the sections were treated with rabbit anti-EGFP (Invitrogen, 1:5,000) to visualize virus expression, and this was followed by ImmPRESS Reagent Kit peroxidase complex (Vector, 1:2). The second immunoperoxidase reaction was developed with DAB as a chromogen (brown reaction product).

In the immunogold staining procedure, following the primary antiserum the sections were incubated in 0.8 nm gold-conjugated goat anti-mouse antibody for vesicular glutamate transporter 2 (vGluT2) (1:50 dilution; Aurion, Wageningen, The Netherlands), overnight at 4°C. Then the sections were silver intensified using the silver enhancement system R-GENT SE-EM according to the kit protocol (Aurion). In the double-immunostaining experiments, the sections were first developed for immunogold and then for immunoperoxidase staining. Lack of cross-reactivity of the secondary antibodies in the sequential detection scheme was verified by omission of either primary antibody, which eliminated labelling by the irrelevant secondary antibody.

After development of the immunostaining, the sections were treated with 1% OsO_4 in 0.1 M PB for 20 min, dehydrated in an ascending series of ethanol and propylene oxide and embedded in Durcupan (ACM; Fluka, Buchs, Switzerland). During dehydration, the sections were treated with 1% uranyl acetate in 70% ethanol for 20 min. From sections embedded in Durcupan, areas of interest were identified by light microscopic examination and then electron microscopic examination was completed. For electron microscopic analysis of the glutamatergic afferents (i.e. mPFC, vHC, BLA, TH) and their postsynaptic targets representative sections of the reconstructed axon arbors were re-embedded and serially sectioned. The terminals found using a Hitachi 7100 electron microscope were photographed, followed in serial sections and their postsynaptic targets were determined.

Postsynaptic targets were determined as VP-projecting neurons if immunoperoxidase reaction end product was diffusely distributed within neuronal somata, as well as in large and small calibre dendritic profiles bearing numerous spines. Spines were identified based on their size and the presence of an asymmetrical input on their heads. The appearance of immunoperoxidase labelling for EGFP (i.e. VP-projecting neurons) was distinct from the gold-silver deposit marking *PHAL*/vGluT2-containing axons, and profiles labelled with immunoperoxidase or silver-gold markers alone were readily distinguishable from each other.

Quantitative analysis of the number of NAc neurons retrogradely labelled from VP

To obtain data on the number of EGFP-positive NAc cells projecting to VP three to four representative sections of the NAc from different Bregma levels (+1.08; 1.68; 2.04; 2.28) were drawn by camera lucida with 6.3× objective. ($n = 4$). In each sample the soma of cells were counted and the cell number was determined per unit area (mm^2) in a 60-μm thick section. The drawings were scaled down and scanned. The area of each region was measured by the NIH ImageJ (US National Institutes of Health, Bethesda, MD) program. In each section the EGFP-positive cells in the

area of NAc were counted and the cell number was determined per unit area (mm^2) in a 60 μm thick section.

Results

Tracer injections

Iontophoretic injection of *Phaseolus vulgaris leucoagglutinin* (*PHAL*) as an anterograde tracer into the region of medial prefrontal cortex (mPFC), basolateral amygdala (BLA) and ventral hippocampus (vHC) produced well-circumscribed, spherical injection sites (Figs. 1A, 2A, 4A, 5A) containing labelled cell bodies and dendrites. *PHAL* was detected in fibres within regions known to receive abundant projections from mPFC, vHC, BLA, including NAc. The topographical distribution of the anterograde labelling from all *PHAL* injection sites was similar to what has been previously reported (Kelley and Domesick 1982; McDonald 1991; Berendse et al. 1992); therefore only a short account is given at the beginning of the respective sections.

To label nucleus accumbens neurons projecting to the VP, AdSynEGFP was used as a retrograde tracer. Within the ventral pallidum (VP), AdSynEGFP injection sites were circumscribed, with viral immunoreactivity in most cases confined to the area immediately adjacent to the injection cannula (Fig. 5A). Only those animals in which AdSynEGFP injection was limited to the VP, and did not infringe on adjacent structures, were included in this study. After AdSynEGFP injection into the VP, numerous neurons (32.9 cells/mm^2) were extensively labelled within the NAc (Figs. 1B, 2B, C, D, 4B, C, D, 5D) Within infected nucleus accumbens-pallidal neurons, immunoreactivity for EGFP was extensively distributed in the soma and throughout the dendritic tree including spines (Figs. 1E, 2E, 4D, 5C). Following virus infection no sign of blebbing or other degenerative processes were seen. In neurons retrogradely labelled by the EGFP-encoded virus from the VP, the immunoperoxidase reaction end product was diffusely distributed within neuronal somata, as well as in large- and small-calibre dendritic profiles bearing numerous spines (Fig. 3C, D, E). The appearance of immunoperoxidase labelling for EGFP was distinct from the gold-silver deposit marking *PHAL*-containing axons, and profiles labelled with immunoperoxidase or silver-gold markers alone were readily distinguishable from each other.

Relationship between *PHAL*-labelled terminals derived from mPFC and retrogradely labelled accumbens-ventral pallidal dendrites

The termination pattern of anterogradely labelled mPFC axons is heterogeneous within the dorsolateral and central parts of the NAc and is largely confined to the core region of the NAc. At higher magnification, the morphology of the anterogradely labelled fibres and varicosities was consistent with previous observations (Groenewegen et al. 1987; Berendse et al. 1992; Wright and Groenewegen 1996), i.e. the mPFC gives rise to a dense network of thin, tortuous fibres that branch frequently and are studded with medium-sized varicosities resulting in a beaded appearance. Such varicosities turned out to be synaptic contacts at the electron microscopic level, consistent with previous reports (Wouterlood and Hrtig 1995). Therefore, these fibres were considered to be potentially in synaptic contact with cells in the NAc. To provide direct evidence for the existence of synaptic connections between *PHAL* labelled fibres and the NAc neurons projecting to the VP, the sections were processed for correlated electron microscopy. In the electron microscope, the gold-silver immunolabelling for *PHAL* was confined to terminals within the NAc, and no soma-dendritic *PHAL* labelling was observed, consistent with the light microscopic observations. *PHAL*-labelled mPFC terminals forming asymmetrical contacts (Fig. 3F) contained clear, round vesicles, which were densely packed, and filled the entire presynaptic bouton, as seen earlier (French and Totterdell 2002).

In double-stained sections we found that even after large *PHAL* injections into the mPFC that resulted in numerous *PHAL*-labelled fibres in NAc, no EGFP immunopositive dendrites or dendritic spines were in synaptic contact with the mPFC afferents. A total of 180 *PHAL*-immunoreactive varicosities (i.e. terminals from mPFC) were examined in single ultrathin sections, and 21 additional varicosities identified by light microscopy were reconstructed from serial EM sections. In spite of all these efforts, no varicosities of *PHAL*-labelled mPFC afferents were found to establish an unequivocal synaptic contact with neurons projecting to VP (i.e. retrogradely labelled for EGFP) in the entire sample, including the random and the light microscopically identified, serially reconstructed terminals. For the 21 potential contacts (adjacent positions of *PHAL* and EGFP-labelled profiles) examined by correlated light and electron microscopy, the dendrites and dendritic spines labelled for EGFP were found to receive innervation only from unlabelled terminals (Fig. 3A, B), whereas the *PHAL*-labelled boutons formed synapses on unlabelled dendrites or spines in the immediate vicinity (Fig. 3F).

Relationship between *PHAL*-labelled terminals derived from vHC and retrogradely labelled accumbens-ventral pallidal dendrites

PHAL-labelled fibres derived from the vHC were unevenly distributed, with most labelled varicosities in the caudal-medial part of the NAc, although a low density of profiles

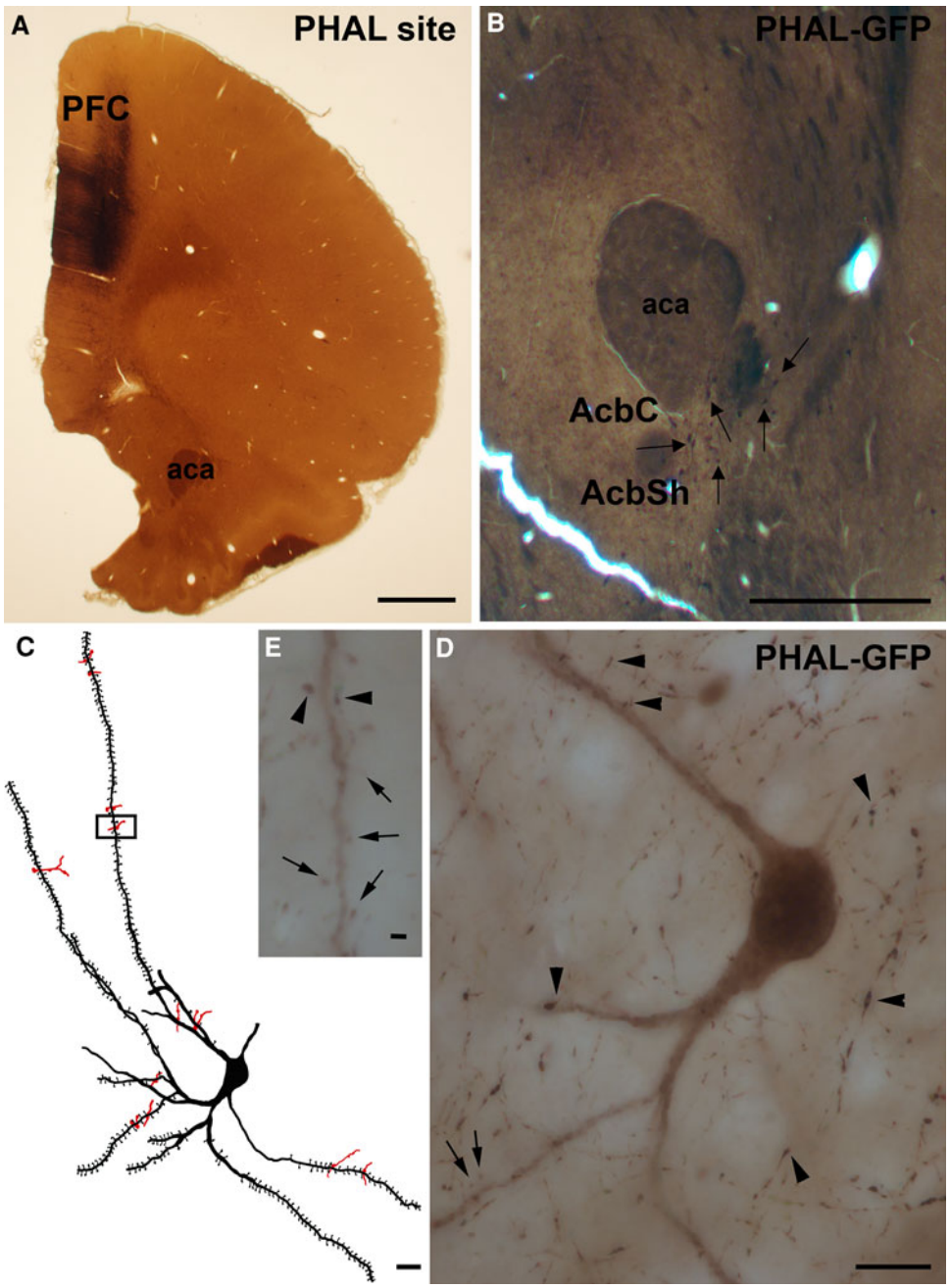

Fig. 1 Light micrograps showing retrograde EGFP labeling and the injection site of *PHAL*. **A** Injection site of *PHAL* that was confined mostly to the prelimbic and infralimbic cortex of PFC. **B** The EGFP immunoreactive neurons retrogradely labelled from the ventral pallidum (VP) in the nucleus accumbens (Acb) (*arrows*). **C**, **D**, **E** Camera lucida drawing and high power light micrographs of EGFP immunopositive cells (*black* and *PHAL*-labelled PFC afferents (*red*). Large boutons (*arrowheads*) of a *PHAL*-labelled PFC axon appear to be in contact with the dendritic shafts or spines (*arrows*) of EGFP-positive neurons in the core region of NAc. These contacts were sampled for correlated electron microscopy. *Scale bars* 1,000 μm (**A**); 500 μm (**B**); 10 μm (**C**, **D**); 1 μm (**E**)

was present throughout the entire rostrocaudal extent of the medial NAc. At rostral levels, anterograde labelling was seen in the dorsomedial aspect of the shell region of the NAc. The vHC gave rise to a less dense innervation compared with the mPFC, possibly because of the relatively smaller number of cells within the vHC that took up the tracer. The vHC fibres were similar in appearance to those derived from the mPFC, i.e. sparsely branching thin fibres were studded with small-to-medium sized varicosities at a relatively low density. Within the NAc, gold-silver deposit—marking *PHAL*-immunostained vHC axons—was confined to axon terminals, no soma-dendritic *PHAL*-labelling was observed, consistent with the light microscopic observations. *PHAL*-labelled boutons contained round clear vesicles that filled most of the axoplasm and rarely contained mitochondria. In double-stained sections, we found that even after large *PHAL* injections into the vHC that resulted in numerous *PHAL*-labelled fibres in NAc, no EGFP immunopositive dendrites or dendritic spines were contacted by the labelled afferents. A total of 102 *PHAL*-immunoreactive varicosities (i.e. terminals from vHC) were examined in single ultrathin sections, and nine additional varicosities in potential contact with EGFP-labelled dendrites as seen in the light microscope were reconstructed from serial ultrathin sections. No

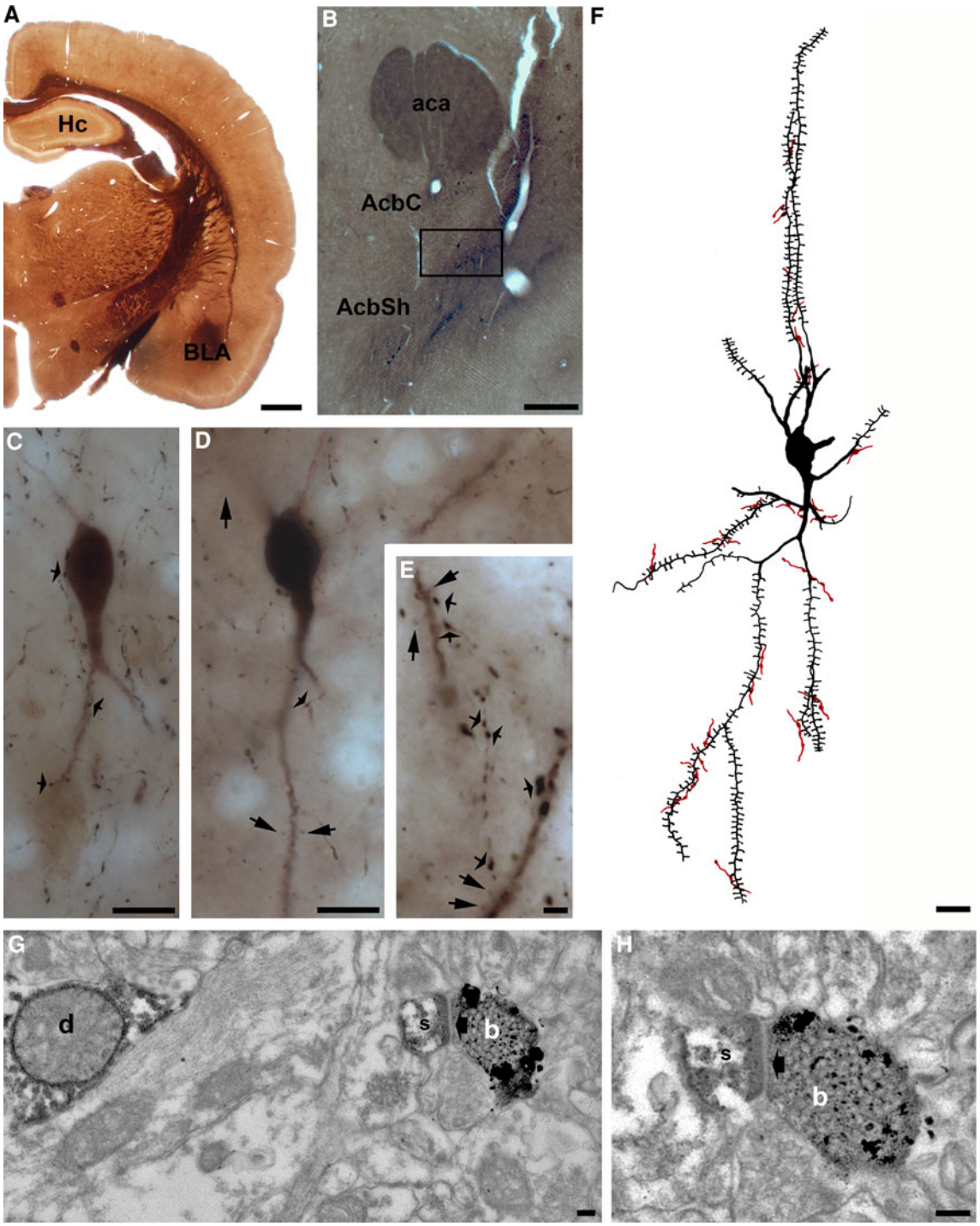

Fig. 2 Axons with large terminals originating from the basolateral amygdaloid nucleus (BLA) establish multiple contacts on EGFP-positive neurons retrogradely labelled from the ventral pallidum (VP). **A** The injection site of *PHAL* was confined to the BLA. **B** The EGFP-immunoreactive neurons retrogradely labelled from the VP in the core and shell region of nucleus accumbens (NAc). **C**, **D**, **E**, **F** Camera lucida drawing and high-power light micrographs of EGFP-positive cells (*black*) with dendrites and dendritic spines (*long arrows*) in the core (**C**) and shell (**D**) of the NAc innervated by *PHAL*-labelled BLA afferents (*red*) (small, *wide arrows*). Several boutons (small, *wide arrows*) are shown to contact the distal dendrites. One of them (b) establishes asymmetrical synaptic contact on the dendritic spine head of the EGFP-positive cell (**G**, **H**). *Scale bars* 1,000 μm (**A**); 200 μm (**B**); 10 μm (**C**, **D**, **F**); 2 μm (**E**); 0.1 μm (**G**, **H**)

PHAL-labelled varicosities of vHC origin were found to establish an unequivocal synaptic contact with neurons projecting to the VP (i.e. retrogradely labelled for EGFP) in the entire sample, including the random and serially reconstructed terminals. Similar to the mPFC samples, the EGFP-labelled dendrites and dendritic spines received

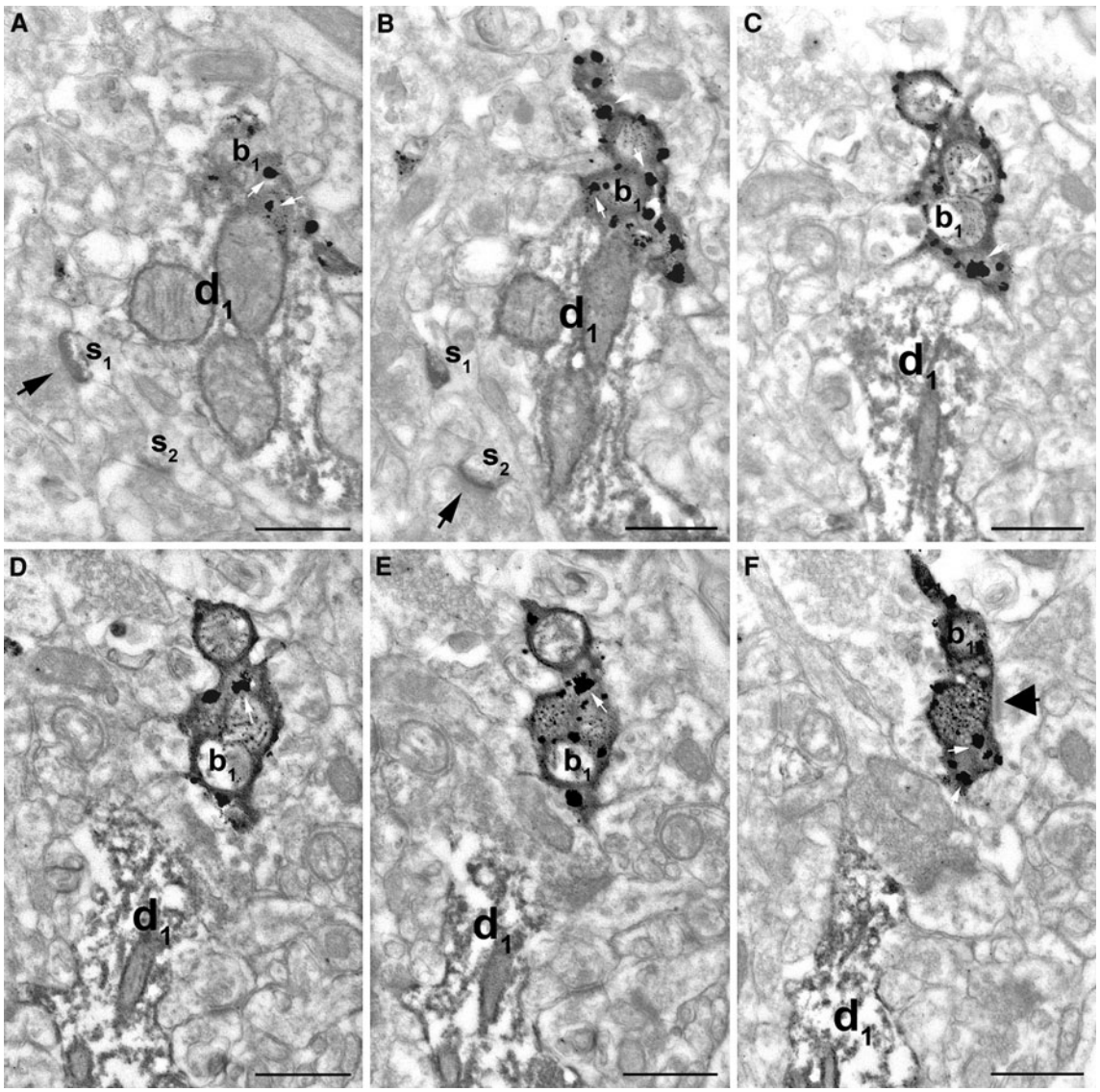

Fig. 3 Electron micrographs of a *PHAL*-labelled bouton anterogradely labelled from PFC correlated in light microscopy (*red* bouton in *black* frame in Fig. 1C). The PFC terminal labelled by silver-intensified gold particles (*white arrows*) forms no synaptic contacts with EGFP-immunoreactive dendrites and spines retrogradely labelled from the ventral pallidum. In **A**–**F**, a *PHAL*-labelled terminal (b_1), shown in serial sections, and forms an asymmetric synaptic contact on an unlabelled dendritic spine (**F**; *arrow*). **A** and **B** show two examples of EGFP-labelled dendritic spines (s_1, s_2) that receive asymmetric synaptic contact from unlabelled terminals (*black arrow*). *PHAL* was visualized with immunoperoxidase staining followed by silver-gold intensification, whereas the EGFP-positive structures by the conventional immunoperoxidase technique using DAB as chromogen. *Scale bars* 0.5 μm (**A**–**F**)

asymmetrical synapses from unlabeled terminals alone, whereas the *PHAL* labelled boutons made contacts on adjacent unlabelled profiles (Fig. 4F_1).

Relationship between terminals derived from BLA and retrogradely labelled accumbens-ventral pallidal dendrites

The *PHAL*-immunoreactive BLA fibres were seen primarily in the caudomedial part of the shell of the NAc, as well as in the adjacent medial part of the core. The rostral half of the NAc also contained some labelled fibres in the extreme dorsomedial corner of the shell. At high magnification, the morphology of the anterogradely labelled fibres and varicosities was consistent with previous observations (Wright and Groenewegen 1996). They are similar in appearance to those derived from the mPFC, i.e. the BLA gives rise to a dense network of thin, tortuous fibres that branch frequently, and are studded with medium-large varicosities giving them a beaded appearance.

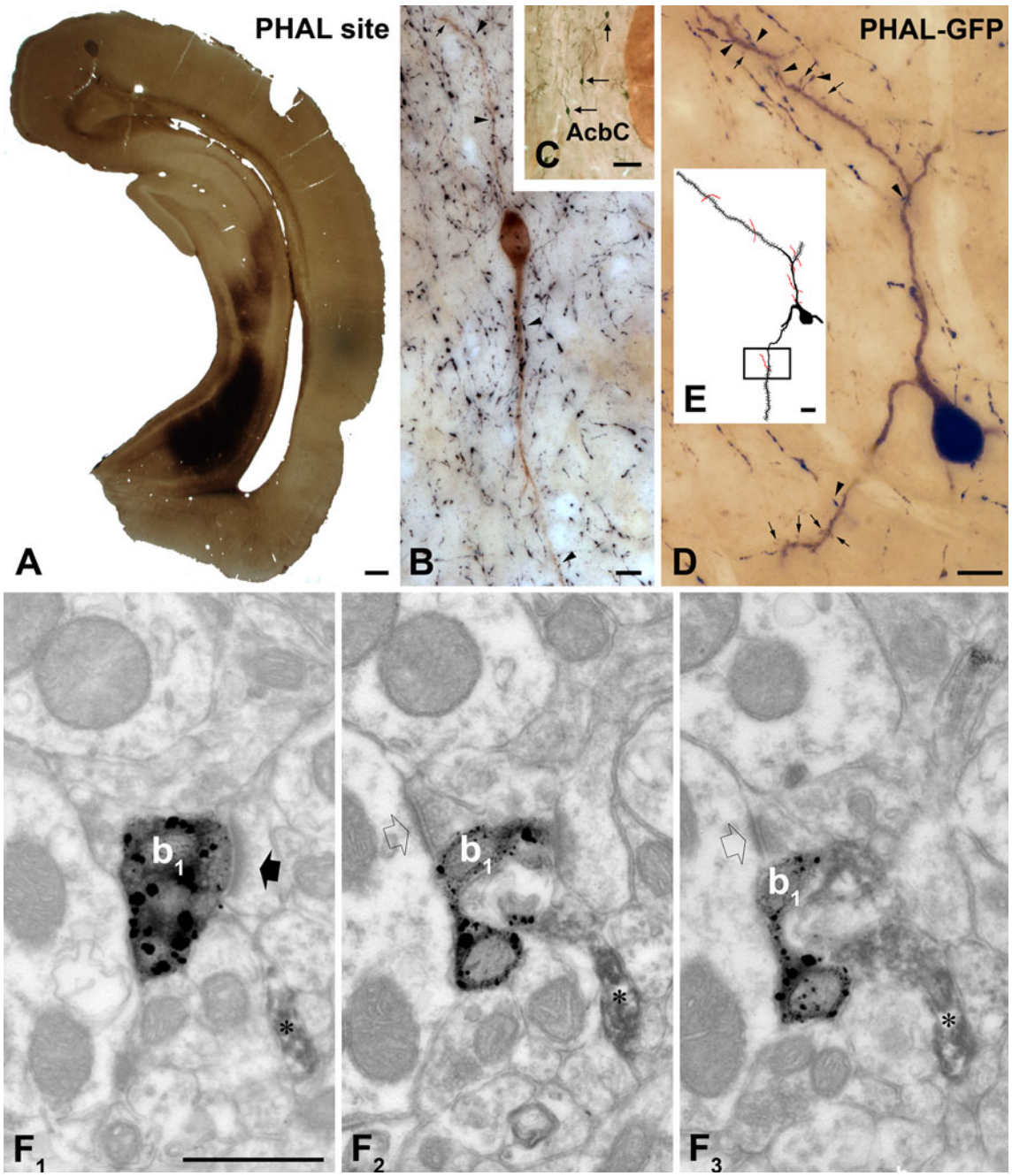

Fig. 4 Correlated light and electron microscopy was used to search for synaptic contacts between EGFP-immunopositive structures retrogradely labelled from VP and anterogradely *PHAL*-labelled axon terminals originating from the ventral hippocampus (vHC). **A** Injection site of *PHAL* confined to the vHC and ventral subiculum. **B** The EGFP-immunoreactive neurons retrogradely labelled from the ventral pallidum (VP) in the nucleus accumbens (NAc). **C**, **D** High-power light micrographs of EGFP-positive cells (*arrows* in **C**) with dendrites and dendritic spines (*arrows* in **D**) that appear to be in contact with large boutons (*arrowheads*) of a *PHAL*-labelled vHC axon in the core region of the NAc. **E** The camera lucida drawing shows that both proximal and distal dendrites as well as dendritic spines were in contact with the *PHAL*-positive boutons (*red*). In $\mathbf{F_1}$, $\mathbf{F_2}$, $\mathbf{F_3}$ a *PHAL*-labelled terminal (in *red* in **E**), is shown in serial sections. It forms no synaptic contact with dendritic spines or shafts of the EGFP-positive neuron. In $\mathbf{F_1}$, bouton b_1 establishes an asymmetric synaptic contact with an unlabeled spine (*black arrow*) *Hollow arrow* shows a synaptic contact between unlabelled bouton and unlabelled dendrite. *Scale bars* 500 μm (**A**); 10 μm (**B**, **D**); 100 μm (**C**); 0.5 μm ($\mathbf{F_1}$–$\mathbf{F_3}$)

Short serial sections cut from 100 varicosities of BLA afferents in 2 animals were examined in the electron microscope; 21 of them were found to form conventional asymmetrical synapses on neurons projecting to the VP. The targets were invariably dendritic spine heads of mostly distal dendrites.

Relationship between retrogradely labelled accumbens-ventral pallidal dendrites and vGluT2 immunolabelled terminals

One of the vesicular glutamate transporters, vGluT2, has been shown to be present mainly in the thalamocortical glutamatergic axons (Kaneko et al. 2002). Since neurons of the (PVT) appear to give rise to the only vGluT2-positive projection to the shell region of NAc (Bubser and Deutch 1998), vGluT2 immunostaining was carried out to label glutamatergic terminals originating from PVT as well as other part of midline and intralaminar thalamus. The distribution pattern of vGluT2 in NAc was similar to that described earlier (Hartig et al. 2003). VGluT2 immunostaining was randomly distributed in the shell region of NAc. (Fig. 5B, C, D). The vGluT2 immunolabelled varicosities contained tightly packed synaptic vesicles, mitochondria, and occasional dense-core vesicles, and mostly targeted dendritic spines, dendritic shafts of various diameter, but rarely somata (Fig. 5F). In double-stained sections, over 100 vGluT2-positive varicosities were examined in 4 animals; 29 of them formed conventional asymmetric synaptic contacts on the dendritic shafts or spines of neurons retrogradely labelled from the VP (Fig. 5F).

Discussion

Both anatomical (French and Totterdell 2002, 2003) and electrophysiological (O'Donnell and Grace 1995) studies have revealed that single neurons in the NAc receive convergent synaptic inputs from limbic structures, such as vHC, BLA and mPFC. The present study, however, represents the first anatomical demonstration of direct glutamatergic synapses onto an identified population of projection neurons in the rat NAc. In particular, we found a selective innervation by BLA and TH of GABAergic medium spiny neurons that project to VP, whereas these were avoided by PFC and vHC afferents.

On a technical note, our results also support the applicability of retrogradely transported AdSynEGFP as a sufficiently sensitive approach to label distal dendrites and dendritic spines of identified projection neurons, thereby facilitating investigations of glutamatergic inputs that typically terminate on these structures. The use of a replication-defective recombinant adenovirus as a vector for the expression of EGFP (under the control of the neuron-specific promoter syn I) allows the retrograde labelling of projection neurons in a Golgi-like manner (Tomioka and Rockland 2006), and it is transported exclusively in the retrograde direction. It can be used in microcircuitry studies in combination with other immunofluorescent stainings or anterograde labelling (Ichinohe et al. 2008).

mPFC and vHC terminals within the NAc

The failure to observe synaptic contacts of mPFC and vHC terminals on the neurons retrogradely labelled from the VP was contrary to our original hypothesis. While it is possible that we missed the mPFC/vHC synaptic contacts on NAc-VP neurons for technical reasons, this seems unlikely given the relatively high density of anterogradely labelled mPFC/vHC terminals, all of which made synaptic contacts on unlabelled dendritic shafts and spines in our material. We conclude that innervation of neurons projecting to VP, if it exists at all, is weak.

The present electron microscopic observations that mPFC and vHC terminals formed exclusively asymmetrical synapses on distal dendrites and dendritic spines are consistent with previous anatomical reports that these pathways likely mediate an excitatory influence on target cells. However, the specific identity of the targeted medium spiny neurons remained unidentified even in the present study.

Our results suggest that the excitatory effect of mPFC/vHC stimulation on medium spiny neurons projecting to VP is not produced by a direct projection from the mPFC or the vHC onto these cells, but rather by an indirect projection, i.e. mPFC/vHC may innervate other neuron types in the NAc that, in turn, terminate on the medium spiny neurons projecting to the VP. These could be the smaller and heterogeneous population of interneurons including fast-spiking GABAergic interneurons and the aspiny cholinergic interneurons, known to play an important role in the integration of NAc functions. The major targets of the mPFC and/or vHC projections in the NAc could be these GABAergic OR cholinergic interneurons OR more likely, since medium spiny projection neurons (MSN) are the most abundant cell type in the NAc, a subset of those MSNs that do not project to the VP (Wilson et al. 1990; Overton et al. 1996; Jackson et al. 2001). The MSNs, in addition to being the principal projection neurons of the NAc, have an extensive recurrent collateral network that arborizes within the NAc (Tunstall et al. 2002). Thus, the function of the mPFC-NAc (and vHC-NAc) innervation could be the modulation of this local circuitry within the NAc, but further investigations are needed to clarify this option. Ultrastructural studies demonstrated that mPFC axons selectively innervate GABA-containing mesoaccumbens (Carr and Sesack 2000) and mesopallidal (Papp E. unpublished observations) neurons within the VTA. Accordingly, the information originating from mPFC can reach the VP via the VTA avoiding the NAc.

Since the mPFC and vHC afferents were found not to provide significant innervation to neurons projecting to VP,

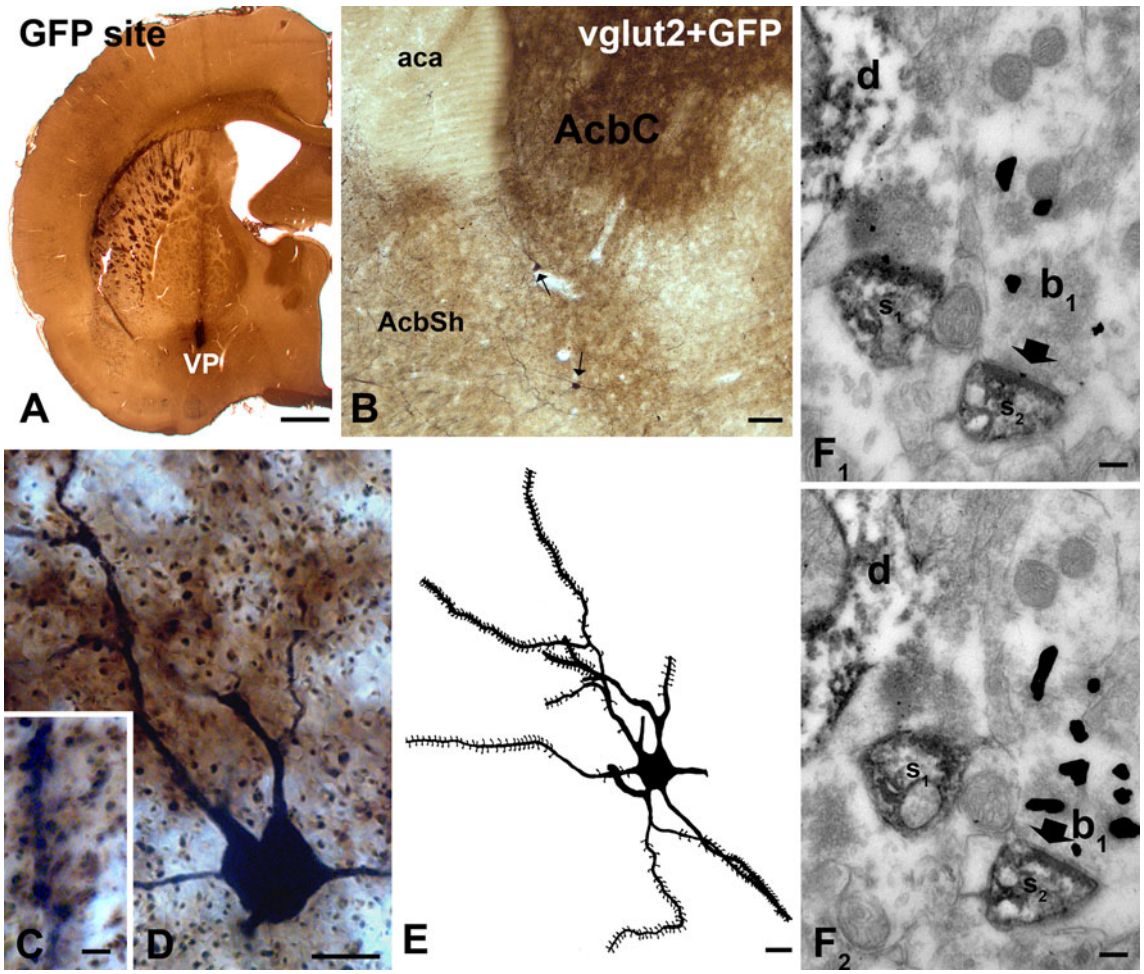

Fig. 5 Light (**A**–**D**) and electron ($\mathbf{F}_1$, $\mathbf{F}_2$) micrographs of sections double-immunostained for vGluT2 and EGFP. VGluT2, as an immunocytochemical marker of glutamatergic afferents originating from the thalamus, was visualized with pre-embedding immunogold (1 nm) staining followed by silver enhancement, whereas EGFP-positive structures by the conventional immunoperoxidase technique using DAB as chromogen. **A** An injection of EGFP was confined to the ventral pallidum (VP). **B** The EGFP-immunoreactive neurons retrogradely labelled from the VP in the core and shell region of nucleus accumbens (NAc) (*arrows*). **C**, **D** Higher-power light micrograph of the NAc shell from the same double-stained section. Several vGluT2-immunopositve boutons are shown to surround the proximal and distal dendrites of the EGFP-immunoreactive neuron. **E** The camera lucida drawing of a EGFP-immunopositive neuron retrogradely labelled from the VP. $\mathbf{F_1}$, $\mathbf{F_2}$ Electron micrographs of a vGluT2-immunoreactive bouton (b_1) establishing synaptic contact (*arrow*) on a dendritic spine of a EGFP-positive neuron in the shell region of NAc. The EGFP immunoreactivity is represented by the diffuse, moderately electron-dense DAB reaction end product, whereas the highly electron-dense granules with sharp contours (silver-enhanced gold particles) signal vGluT2-immunoreactivity. *Scale bars* 1,000 μm (**A**); 100 μm (**B**); 10 μm (**D**, **E**); 2 μm (**C**); 0.1 μm ($\mathbf{F}_1$, $\mathbf{F}_2$)

they could use the direct VTA pathway to influence VTA neurons (mPFC-VTA and/or vHC-VTA). Previous studies revealed the presence of a projection from the NAc to the VTA avoiding the VP (Kalivas et al. 1993). Thus, the medium spiny neurons of NAc receiving mPFC or vHC input could also control VTA neurons via the direct NAc-VTA route.

BLA and TH terminals within the NAc

We provided structural evidence that the NAc-VP pathway is under the direct synaptic control of excitatory inputs coming from the BLA and TH. The TH/BLA glutamatergic pathways can initiate neuronal firing in the NAc, which, in turn, inhibits the VP and release dopamine neurons from inhibition within the VTA (McDonald 1991; Usuda et al. 1998; Grace et al. 2007). Ultrastructural studies reported that PVT terminals are often found in the immediate vicinity of dopamine (DA) terminals in the NAc shell region, which led the authors to speculate that glutamate released from TH afferents could directly regulate the level of DA via glutamate receptors located on DA terminals (Pinto et al. 2003). In addition, the same study suggests that the TH axons could control DA levels within the NAc also

via the TH-NAc-(VP-)-VTA-NAc route. The synaptic convergence onto common targets by PVT terminals and DA axons has been reported in the NAc, but not the PFC (Pinto et al. 2003). Data show that the NAc inputs coming from the limbic system and PFC are differentially regulated by dopamine receptor subtypes. The activation of BLA and TH drives neuronal firing in the NAc, which, in turn, likely inhibits the VP and releases dopamine neurons from inhibition (indirect route: NAc-VP-VTA). On the other hand, the mPFC/vHC glutamatergic route may be responsible for inhibiting dopamine neurons in the VTA via a direct route (NAc-VTA); that is GABAergic and enkephalinergic NAc neurons project to the VTA (Kalivas et al. 1993).

Functional implications

Physiological data have indicated an influence of inactivation of the VP—by stimulation of the vHC (that activates the NAc-VP GABA pathway)—increases tonic activity of DA neurons in the VTA, which causes an increase in extracellular DA levels in the NAc (Floresco et al. 2003). Inactivation of VP attenuates PFC-evoked responses, whereas VP activation facilitates PFC-evoked responses in NAc through D2 receptors (Goto and Grace 2005). The data obtained in our study, however, suggest that these effects operate via an indirect excitatory projection from mPFC/vHC to NAc neurons projecting to the VP.

Different ensembles of NAc neurons appear to be activated by different combinations of inputs and project to various targets. This input–output pattern could play an important role in behaving animals to adapt to different environmental conditions.

The dopamine neurons show behaviour-related phasic activation following various environmental stimuli with positive motivational value, without distinguishing these effects. Neurons in other brain structures such as the NAc and amygdala discriminate between various rewards (Schultz 2002). The glutamatergic inputs of different origin (i.e. mPFC, vHC, BLA, PVN) to the NAc might thus convey different types of reward-related information during goal-directed behaviour and thereby contribute to the complex regulation of nucleus accumbens functions.

Acknowledgments This work was supported by a NIH NS030549, NIH DA09158, EU GENADDICT LSHM-CT-2004-005166, NKTH-OTKA, CNK77793, HHMI 55005608 grants. The excellent technical assistance of E. Simon Szépné and Gy. Goda is also acknowledged. E. P. is a grantee of the János Bólyai scholarship.

References

Berendse HW, Galis-de Graaf Y, Groenewegen HJ (1992) Topographical organization and relationship with ventral striatal compartments of prefrontal corticostriatal projections in the rat. J Comp Neurol 316:314–347

Bhatnagar S, Dallman MF (1999) The paraventricular nucleus of the thalamus alters rhythms in core temperature and energy balance in a state-dependent manner. Brain Res 851:66–75

Bhatnagar S, Viau V, Chu A, Soriano L, Meijer OC, Dallman MF (2000) A cholecystokinin-mediated pathway to the paraventricular thalamus is recruited in chronically stressed rats and regulates hypothalamic-pituitary-adrenal function. J Neurosci 20:5564–5573

Bubser M, Deutch AY (1998) Thalamic paraventricular nucleus neurons collateralize to innervate the prefrontal cortex and nucleus accumbens. Brain Res 787:304–310

Carr DB, Sesack SR (2000) Projections from the rat prefrontal cortex to the ventral tegmental area: target specificity in the synaptic associations with mesoaccumbens and mesocortical neurons. J Neurosci 20:3864–3873

DeFrance JF, Marchand JF, Sikes RW, Chronister RB, Hubbard JI (1985) Characterization of fimbria input to nucleus accumbens. J Neurophysiol 54:1553–1567

Deutch AY, Bubser M, Young CD (1998) Psychostimulant-induced Fos protein expression in the thalamic paraventricular nucleus. J Neurosci 18:10680–10687

Dobo E, Takacs VT, Gulyas AI, Nyiri G, Mihaly A, Freund TF (2011) New silver-gold intensification method of diaminobenzidine for double-labeling immunoelectron microscopy. J Histochem Cytochem 59:258–269

Fanselow MS, Dong, HW (2010) Are the dorsal and ventral hippocampus functionally distinct structures? Neuron 65:7–19

Floresco SB, West AR, Ash B, Moore H, Grace AA (2003) Afferent modulation of dopamine neuron firing differentially regulates tonic and phasic dopamine transmission. Nat Neurosci 6:968–973

French SJ, Totterdell S (2002) Hippocampal and prefrontal cortical inputs monosynaptically converge with individual projection neurons of the nucleus accumbens. J Comp Neurol 446:151–165

French SJ, Totterdell S (2003) Individual nucleus accumbens-projection neurons receive both basolateral amygdala and ventral subicular afferents in rats. Neuroscience 119:19–31

Fuller TA, Russchen FT, Price JL (1987) Sources of presumptive glutamergic/aspartergic afferents to the rat ventral striatopallidal region. J Comp Neurol 258:317–338

Gerfen CR, Sawchenko PE (1984) An anterograde neuroanatomical tracing method that shows the detailed morphology of neurons, their axons and terminals: immunohistochemical localization of an axonally transported plant lectin, Phaseolus vulgaris leucoagglutinin (PHA-L). Brain Res 290:219–238

Goto Y, Grace AA (2005) Dopaminergic modulation of limbic and cortical drive of nucleus accumbens in goal-directed behavior. Nat Neurosci 8:805–812

Grace AA, Floresco SB, Goto Y, Lodge DJ (2007) Regulation of firing of dopaminergic neurons and control of goal-directed behaviors. Trends Neurosci 30:220–227

Groenewegen HJ, Becker NE, Lohman AH (1980) Subcortical afferents of the nucleus accumbens septi in the cat, studied with retrograde axonal transport of horseradish peroxidase and bisbenzimid. Neuroscience 5:1903–1916

Groenewegen HJ, Vermeulen-Van der Zee E, te Kortschot A, Witter MP (1987) Organization of the projections from the subiculum to the ventral striatum in the rat. A study using anterograde transport of Phaseolus vulgaris leucoagglutinin. Neuroscience 23:103–120

Groenewegen HJ, Berendse HW, Haber SN (1993) Organization of the output of the ventral striatopallidal system in the rat: ventral pallidal efferents. Neuroscience 57:113–142

Haber SN, Groenewegen HJ, Grove EA, Nauta WJ (1985) Efferent connections of the ventral pallidum: evidence of a dual striato pallidofugal pathway. J Comp Neurol 235:322–335

Hartig W, Riedel A, Grosche J, Edwards RH, Fremeau RT Jr, Harkany T, Brauer K, Arendt T (2003) Complementary distribution of vesicular glutamate transporters 1 and 2 in the nucleus accumbens of rat: relationship to calretinin-containing extrinsic innervation and calbindin-immunoreactive neurons. J Comp Neurol 465:1–10

Heimer L, Zaborszky L, Zahm DS, Alheid GF (1987) The ventral striatopallidothalamic projection: I. The striatopallidal link originating in the striatal parts of the olfactory tubercle. J Comp Neurol 255:571–591

Ichinohe N, Hyde J, Matsushita A, Ohta K, Rockland KS (2008) Confocal mapping of cortical inputs onto identified pyramidal neurons. Front Biosci 13:6354–6373

Jackson ME, Frost AS, Moghaddam B (2001) Stimulation of prefrontal cortex at physiologically relevant frequencies inhibits dopamine release in the nucleus accumbens. J Neurochem 78:920–923

Jongen-Relo AL, Voorn P, Groenewegen HJ (1994) Immunohistochemical characterization of the shell and core territories of the nucleus accumbens in the rat. Eur J Neurosci 6:1255–1264

Kalivas PW, Churchill L, Klitenick MA (1993) GABA and enkephalin projection from the nucleus accumbens and ventral pallidum to the ventral tegmental area. Neuroscience 57:1047–1060

Kaneko T, Fujiyama F, Hioki H (2002) Immunohistochemical localization of candidates for vesicular glutamate transporters in the rat brain. J Comp Neurol 444:39–62

Kelley AE, Berridge KC (2002) The neuroscience of natural rewards: relevance to addictive drugs. J Neurosci 22:3306–3311

Kelley AE, Domesick VB (1982) The distribution of the projection from the hippocampal formation to the nucleus accumbens in the rat: an anterograde- and retrograde-horseradish peroxidase study. Neuroscience 7:2321–2335

Koob GF, Bloom FE (1988) Cellular and molecular mechanisms of drug dependence. Science 242:715–723

McDonald AJ (1991) Organization of amygdaloid projections to the prefrontal cortex and associated striatum in the rat. Neuroscience 44:1–14

Mogenson GJ, Jones DL, Yim CY (1980) From motivation to action: functional interface between the limbic system and the motor system. Prog Neurobiol 14:69–97

O'Donnell P, Grace AA (1993) Physiological and morphological properties of accumbens core and shell neurons recorded in vitro. Synapse 13:135–160

O'Donnell P, Grace AA (1995) Synaptic interactions among excitatory afferents to nucleus accumbens neurons: hippocampal gating of prefrontal cortical input. J Neurosci 15:3622–3639

O'Donnell P, Grace AA (1998) Dysfunctions in multiple interrelated systems as the neurobiological bases of schizophrenic symptom clusters. Schizophr Bull 24:267–283

Overton PG, Tong ZY, Clark D (1996) A pharmacological analysis of the burst events induced in midbrain dopaminergic neurons by electrical stimulation of the prefrontal cortex in the rat. J Neural Transm 103:523–540

Paxinos G, Watson C (1998) The rat brain in stereotaxic coordinates. Academic Press, New York

Pinto A, Jankowski M, Sesack SR (2003) Projections from the paraventricular nucleus of the thalamus to the rat prefrontal cortex and nucleus accumbens shell: ultrastructural characteristics and spatial relationships with dopamine afferents. J Comp Neurol 459:142–155

Schultz W (2002) Getting formal with dopamine and reward. Neuron 36:241–263

Sloviter RS, Ali-Akbarian L, Horvath KD, Menkens KA (2001) Substance P receptor expression by inhibitory interneurons of the rat hippocampus: enhanced detection using improved immunocytochemical methods for the preservation and colocalization of GABA and other neuronal markers. J Comp Neurol 430:283–305

Tomioka R, Rockland KS (2006) Improved Golgi-like visualization in retrogradely projecting neurons after EGFP-adenovirus infection in adult rat and monkey. J Histochem Cytochem 54:539–548

Tunstall MJ, Oorschot DE, Kean A, Wickens JR (2002) Inhibitory interactions between spiny projection neurons in the rat striatum. J Neurophysiol 88:1263–1269

Usuda I, Tanaka K, Chiba T (1998) Efferent projections of the nucleus accumbens in the rat with special reference to subdivision of the nucleus: biotinylated dextran amine study. Brain Res 797:73–93

Wilson CJ, Chang HT, Kitai ST (1990) Firing patterns and synaptic potentials of identified giant aspiny interneurons in the rat neostriatum. J Neurosci 10:508–519

Wouterlood FG, Hrtig W (1995) Calretinin-immunoreactivity in mitral cells of the rat olfactory bulb. Brain Res 682:93–100

Wright CI, Groenewegen HJ (1996) Patterns of overlap and segregation between insular cortical, intermediodorsal thalamic and basal amygdaloid afferents in the nucleus accumbens of the rat. Neuroscience 73:359–373

Young CD, Deutch AY (1998) The effects of thalamic paraventricular nucleus lesions on cocaine-induced locomotor activity and sensitization. Pharmacol Biochem Behav 60:753–758